

## Phonon localization in periodic uniaxially nanostructured silicon

Sylvain G. Cloutier,<sup>a)</sup> Rodney S. Guico, and Jimmy M. Xu

Division of Engineering and Department of Physics, Brown University, Providence, Rhode Island 02912

(Received 14 July 2005; accepted 14 October 2005; published online 21 November 2005)

Phonon spectroscopy of low-dimensional silicon nanostructures may help identify and understand their unique physical properties for potentially enabling new applications. High-resolution Raman spectroscopy reveals that fabrication of such nanostructures can lead to the creation of nanosize crystallites at the silicon interface due to the introduction of defect centers which is most likely responsible for local crystal-symmetry breaking and phonon localization. By examining these nanocrystallites created in periodic crystalline silicon nanodot arrays formed in silicon-on-insulator and their dispersive and power-dependent phonon spectra, we found clear evidence of spatial phonon localization, which in turn suggests a breaking of the fundamental phonon-selection rule limiting radiative recombination in silicon's indirect band structure. © 2005 American Institute of Physics. [DOI: 10.1063/1.2135881]

Persistent efforts have been made to enhance light emission from silicon,<sup>1</sup> which is fundamentally limited by its indirect band structure where radiative recombination is strongly disfavored by the large  $k$  mismatch between the available electron and hole states and competition with a myriad of faster nonradiative processes. As such, light emission is allowed only if a phonon matching the crystal's momentum is absorbed or emitted in the recombination process. One way to break this phonon-selection rule would be via symmetry breaking and phonon localization.<sup>2,3</sup> Two conceptually valid ways to generate such effect rely on phonon confinement in silicon nanocrystals<sup>3-5</sup> or a high concentration of defect centers in the crystalline silicon.<sup>2,6,7</sup> Phonon confinement in silicon nanocrystals and nanowires continues to be widely studied and is now relatively well understood.<sup>5,8-11</sup> In the present work, we use high-resolution phonon spectroscopy to reveal the creation of nanosized crystallites at the silicon nanodot surface acting as phonon-localization centers and leading to a breaking of the fundamental phonon-selection rule in this indirect-band gap semiconductor.

The periodic array of silicon nanodot structures shown in Fig. 1(a) was formed in undoped crystalline 205-nm-thick electronic-grade silicon-on-insulator (SOI) using a highly uniform self-organized nanopore array as a mask. The anodic aluminum oxide (AAO) nanopore mask was fabricated in a two-step anodization process under conditions previously described.<sup>12-14</sup> Grown to a 750 nm thickness, such a nanopore mask was placed atop the SOI layer, which is insulated from the thick silicon substrate by 3  $\mu\text{m}$  of silicon-oxide. The silicon nanodot array was obtained by first using the AAO as a metal-evaporation mask and then proceeding with chlorine-based reactive ion etching (RIE) after AAO removal, using the electron-beam evaporated metal nanodots as the etching mask.

High-resolution phonon-spectroscopy measurements were performed using a ThermoNicolet Almega Raman microscope equipped with a high-resolution motorized stage and two excitation laser sources emitting at 532 and 785 nm. At a 100 $\times$  magnification, with the excitation spot diameter

being  $\approx 1 \mu\text{m}$  and the SOI insulation layer being 3  $\mu\text{m}$  thick, the setup allows cross-sectional measurement of the top-most silicon layer as shown in Fig. 1(b). Figure 1 compares the Raman spectra obtained this way for bulk undoped silicon  $\langle 100 \rangle$ , original unpatterned SOI and the silicon nanodot array on SOI. The measurements were performed using the 532 nm laser with a 20.4 mW laser power and were integrated over 200 scans.

Compared with the bulk silicon, the original unpatterned SOI spectrum shows asymmetric broadening and a slight shift towards lower wave numbers, which can be attributed to tensile and/or compressive strain in the SOI.<sup>15</sup> However, the combined large downshift in wave number and the additional asymmetric broadening observed for the silicon nanodot array on SOI can not be explained by strains only, nor can it be explained by the high density of photogenerated electrons or Fano resonances since the electron concentration required to justify such a shift would be unreasonably high.<sup>7,9</sup>

It has been established both in earlier theories and experiments that phonon confinement on scale sizes smaller than  $\approx 10 \text{ nm}$  could lead to such combined significant downshift and asymmetric broadening of silicon's optical-phonon peak.<sup>4,5</sup> The downshift and broadening of the phonon line in

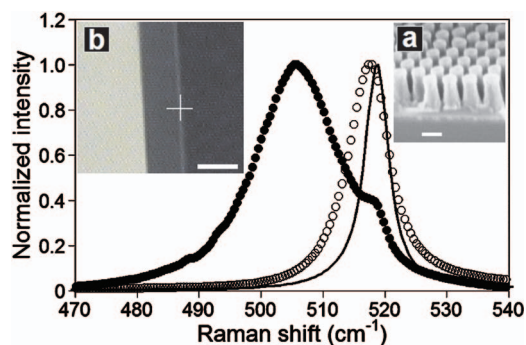


FIG. 1. (Color) Raman spectra measured from bulk undoped silicon (—), original unpatterned SOI (○), and the silicon nanodot array on SOI (●). Insets: (a) 60° cross-sectional scanning electron microscopy view of the silicon nanodot array on SOI. The scale bar is 100 nm. (b) Raman-microscope cross-sectional view of a SOI sample. The cross indicates the optically excited top-layer region. The scale bar is 3  $\mu\text{m}$ .

<sup>a)</sup>Electronic mail: sylvain\_cloutier@brown.edu

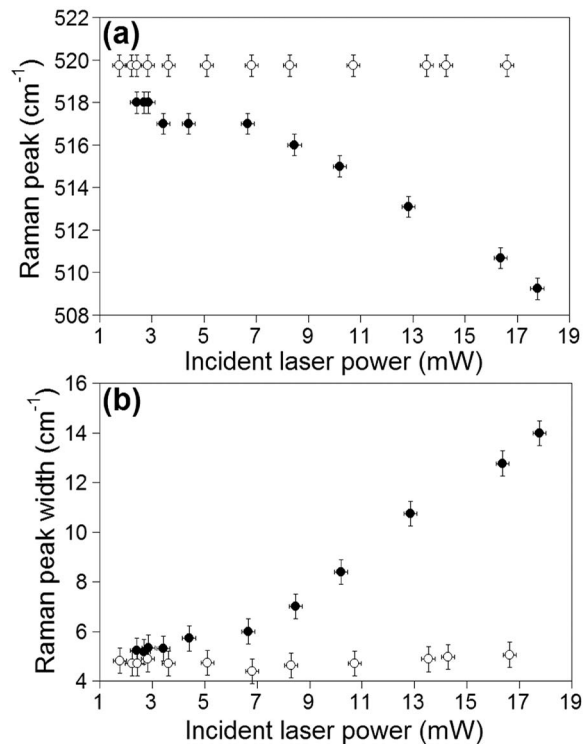


FIG. 2. Raman-shift peak (a) spectral position and (b) width as a function of the excitation power for the silicon nanodot array on SOI. Dispersive measurements were performed using both the 532 nm (●) and the 785 nm (○) laser sources.

such confined silicon structures can be explained by the partial breakdown of the Raman-selection rule attributed to phonon-localization effects.<sup>4</sup> It was also experimentally established that this combined shift and broadening should be both dispersive and excitation-power dependent.<sup>9,11</sup>

Figure 2 shows the downshift and the broadening of the main phonon line as a function of the incident laser power for the silicon nanodot array on SOI using both the 532 nm and the 785 nm excitation sources. The results clearly show an increased downshift and broadening as the 532 nm excitation-power is increased. However, the 785 nm excitation appears to generate little or no additional shift or broadening with increasing laser power, in good agreement with previous results on phonon-confinement effects in silicon nanocrystals.<sup>9,11</sup>

One factor yet to be taken into account is the laser-induced self-heating effect. It has been indeed demonstrated that laser heating of bulk silicon can lead to an additional downshift of its phonon line.<sup>9</sup> Therefore, it is of critical importance to distinguish the contribution of the phonon-confinement effect from the self-heating one. An easy way to probe the laser-induced heating is to record simultaneously the Stokes (+520 cm<sup>-1</sup>) and anti-Stokes (-520 cm<sup>-1</sup>) vibrational lines in the Raman spectra as shown in the inset of Fig. 3. The intensity ratio of these two phonon lines can be related to the sample temperature  $T$  by the well-known relation  $I_S/I_{AS} \approx \exp(-E_p/kT)$ , where  $I_S$  and  $I_{AS}$  are the intensities of the Stokes and anti-Stokes vibrational lines respectively,  $E_p$  is the phonon energy, and  $k$  is the Boltzman constant. For silicon,  $E_p \approx 64.47$  meV (determined from the position of the main phonon line). By monitoring the change in the Stoke/anti-Stokes intensity ratio while varying the incident excitation power, we were able to determine *in situ* the temperature

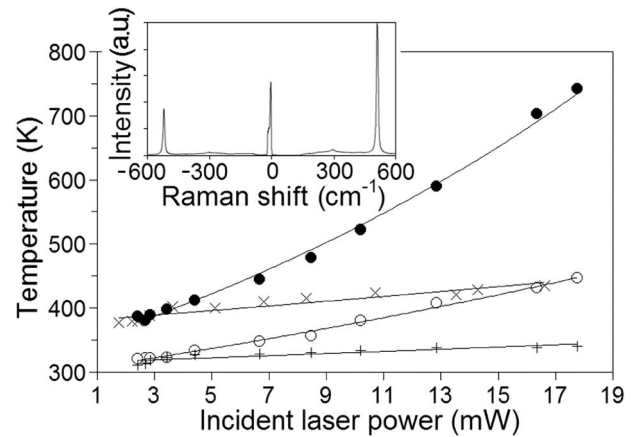


FIG. 3. Sample temperature as a function of the incident 532 nm laser power for bulk silicon (+), original unpatterned SOI (○), and the silicon nanodot array on SOI (●). Also plotted is the temperature evolution of the nanodots with increasing excitation power measured using the 532 nm (●) and the 785 nm (×) laser sources. Inset: Raman-shift spectra displaying the Stokes and anti-Stokes phonon lines for the nanodots on SOI under a 17.8 mW excitation at 532 nm.

evolution for each sample. Figure 3 displays the temperature evolution measured for the silicon nanodot array on SOI, original unpatterned SOI, and bulk silicon while varying the 532 nm excitation power. The results clearly demonstrate increased heating while reducing the effective dimensionality, as one may anticipate based on the change in thermal mass and conductance. SOI heats up more than the bulk silicon since its capacity to dissipate heat is limited to two-dimensions while the silicon nanodots on SOI show the highest laser-induced heating due to the lowest thermal mass and limited heat dissipation in all directions. Moreover, the 532 nm laser heats the nanodot sample more than the 785 nm as shown in Fig. 3, which seems to provide a possible explanation for the dispersive dependence observed in Fig. 2.

The phonon-peak downshift as a function of its associated width (i.e., shift-width evolution) can also be plotted and the results are shown in Fig. 4. The clear nonlinear evolution region observed at low excitation power (or low sample temperature), indicates that the phonon-line downshifts and broadens at different rates as the excitation power is increased, a clear signature of phonon-localization effects.<sup>5</sup> At higher excitation powers, the shift-width evolution be-

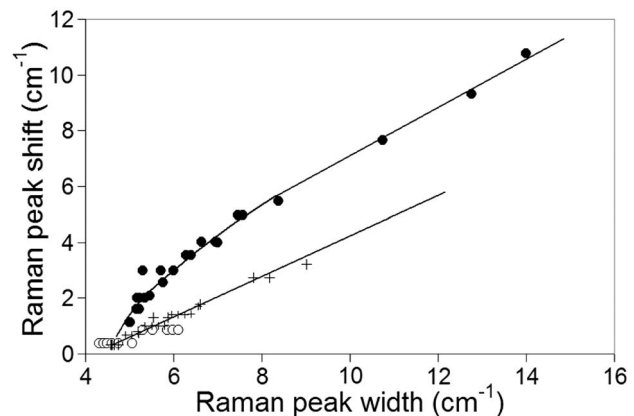


FIG. 4. Raman-peak downshift as a function of the associated width for the nanostructured (●) and unpatterned SOI (○). Also plotted are the results obtained for the same nanostructured SOI sample after a short (8 min) thermal oxidation at 980 °C (+).

comes linear marking out a laser-heating dominated regime.

However, the apparent features sizes ( $\approx 70$  nm) are much too large to explain such phonon-localization effects,<sup>5</sup> suggesting that localization may have taken place in substructures. One hypothesis would be the presence of nanocrystallite domains created at the nanodot surface during the RIE, which is plausible given that the RIE process is known to introduce surface defects. In such substructures, phonon localization may occur in a way similar to the suggested process for phonon confinement and long-range symmetry breaking due to high local defect-centers concentration.<sup>2,6,7</sup> Therefore, these nanocrystallites would locally act as phonon-localization centers. Since RIE is a relatively low-energy process, such defect centers would be located mostly in the nanostructured-silicon surface layer. The high surface-to-volume ratio in the periodic nanodot array on SOI would indeed allow observation of this effect using high-resolution Raman spectroscopy.

To verify this hypothesis, we thermally oxidized the SOI nanodots at 980 °C for 8 min, which resulted in oxidizing a 4–6 nm layer at the silicon-dot surface. Figure 4 compares the shift-width evolution from the same nanostructured SOI sample before and after oxidation. After the thermal treatment, the nonlinear-evolution region disappeared and the shift-width evolution becomes linear with a slightly decreased slope, similar to the results obtained for original unpatterned SOI, which suggests the removal of any phonon-localization effect. This confirms that the phonon-localization effect observed is most likely due to the presence of nanosized crystallites at the nanostructured silicon interface which were removed by the fast thermal-oxidation process.

In summary, we observed and studied phonon-localization effects in periodic uniaxially nanostructured silicon nanodot array fabricated using a highly ordered array of nanopores as a mask. The conventional chlorine-based RIE process used to etch the nanosized dots into crystalline SOI apparently leads to the creation of nanocrystallites in the silicon dots which are responsible for phonon-localization effects observed using high-resolution Raman spectroscopy. A

brief thermal-oxidation was performed which removed any such effect, suggesting that those nanoscale crystallites are most-likely located in the nanostructured-silicon surface layer and are acting as phonon-localization centers which break the fundamental phonon-selection rule taking place in bulk silicon and would in turn favor radiative recombination and light emission. Given the importance of the breaking of the phonon-selection rules associated with phonon-localization to achieve light-emission enhancement in silicon and other indirect-band gap materials,<sup>3</sup> we believe the findings presented here provide physical insight and offer useful guidelines to controllably modify the optical properties of indirect semiconductors through defect engineering.

The authors acknowledge support from ONR and DARPA. S.G.C. and J.M.X. are thankful to NSERC and the Guggenheim Foundation, respectively, for the fellowship supports.

<sup>1</sup>L. Pavesi, S. Gaponenko, and L. Dal Negro, *Towards the First Silicon Laser* (Kluwer Academic, Dordrecht, 2003).

<sup>2</sup>P. T. Landsberg, *Solid-State Electron.* **10**, 513 (1967).

<sup>3</sup>D. Kovalev, H. Heckler, G. Polisski, and F. Koch, *Phys. Status Solidi B* **215**, 871 (1999).

<sup>4</sup>H. Richter, Z. P. Wang, and L. Ley, *Solid State Commun.* **39**, 625 (1981).

<sup>5</sup>I. H. Campbell and P. M. Fauchet, *Solid State Commun.* **58**, 739 (1986).

<sup>6</sup>M. Chandrasekhar, H. R. Chandrasekhar, M. Grimsditch, and M. Cardona, *Phys. Rev. B* **22**, 4825 (1980).

<sup>7</sup>N. H. Nickel, P. Lengsfeld, and I. Sieber, *Phys. Rev. B* **61**, 15558 (2000).

<sup>8</sup>J. Zi, H. Buscher, C. Falter, W. Ludwig, K. Zhang, and X. Xie, *Appl. Phys. Lett.* **69**, 200 (1996).

<sup>9</sup>S. Piscanec, M. Cantoro, A. C. Ferrari, J. A. Zapien, Y. Lifshitz, S. T. Lee, S. Hofmann, and J. Robertson, *Phys. Rev. B* **68**, 241312 (2003).

<sup>10</sup>M. S. Hybertsen, *Phys. Rev. Lett.* **72**, 1514 (1994).

<sup>11</sup>N. Fukata, T. Oshima, K. Murakami, T. Kizuka, T. Tsurui, and S. Ito, *Appl. Phys. Lett.* **86**, 213112 (2005).

<sup>12</sup>J. Liang, H. Chik, A. Yin, and J. Xu, *J. Appl. Phys.* **91**, 2544 (2002).

<sup>13</sup>A. P. Li, F. Müller, A. Birner, K. Nielsch, and U. Gösele, *J. Appl. Phys.* **84**, 6023 (1998).

<sup>14</sup>H. Masuda, H. Yamada, M. Satoh, H. Asoh, M. Nakao, and T. Tamamura, *Appl. Phys. Lett.* **71**, 2770 (1997).

<sup>15</sup>J. Camassel, L. A. Falkovsky, and N. Planes, *Phys. Rev. B* **63**, 035309 (2000).